Sodium tanshinone IIA sulfonate inhibits proliferation, migration, invasion and inflammation in rheumatoid arthritis fibroblast-like synoviocytes

Zeyu Wang, Jinglong Li, Jun Zhang, Xuhua Xie*

Department of Orthopedics, The First People's Hospital of Yunnan Province, the People's Republic of China

ARTICLE INFO

ABSTRACT

Our study aimed to determine the effects of sodium tanshinone IIA sulfonate (STS) on proliferation, migration, invasion, and inflammation in rheumatoid arthritis human fibroblast-like synoviocytes (RA-HFLSs). Firstly, results demonstrated STS reduced proliferation, migration, invasion in HFLSs. Also, we found that STS could alleviate the reorganizations of F-actin cytoskeleton in TNF-α-treated HFLSs. In addition, STS decreased the production of IL-1β, IL-6, MMP-1, and MMP-3 in TNF-α-treated RA-HFLSs. Further study showed that STS blocked MAPK/NF-κB activations in TNF-α-stimulated RA-HFLSs. Moreover, we illustrated that STS could alleviate rheumatoid arthritis progression and prevent inflammation damage in joint tissues of collagen-induced arthritis (CIA) mice. Taken together, this study suggested that STS inhibited proliferation, migration, invasion, and inflammation of RA-HFLSs by blocking MAPK/NF-κB pathways.

1. Introduction

Rheumatoid arthritis (RA) is a chronical and systemic autoimmune disease [1,2]. It is well known that RA is distinguished by synovitis inflammation, synovial hyperplasia and the progressive destruction of cartilage and joints [1–3]. The rheumatoid arthritis fibroblast like synoviocytes (RA-FLSs) that locate at the synovial intimal edges is resident mesenchymal cells [4,5]. The activated RA-FLSs play an important role in the inflammatory response, synovial hyperplasia, joint destruction, and comorbidity in the RA progression [6,7]. Accumulating evidence indicate that RA-FLSs could be activated and display tumor cells-like biological characteristics, like aggressive proliferation, migration, and invasion, which contributes to damages of cartilage, joint, and bone. In addition, the RA-FLSs could also produce and secrete inflammatory cytokines, which could deteriorate the RA progression as feedback [4,5]. Therefore, modulating RA-FLSs proliferation, migration, and invasion and RA-FLSs-induced inflammatory process might be therapeutic strategies for RA treatments.

Tanshinone IIA (TIIA) is one of the main pharmacological components of the famous herbal medicine, *Salvia miltiorrhiza* that has been widely used for cardiovascular diseases treatment in China [8–12]. Sodium tanshinone IIA sulfonate (STS), a water-soluble sulfonate derived from TIIA, has been approved by the State Food and Drug Administration of China (CFDA) for treating coronary heart disease and ischemic stroke [8–12]. Accumulating evidence demonstrates inhibitory STS-mediated effects against inflammation and oxidative stress contributes to its protections on cardiovascular diseases [8–12]. Previous studies have also found that STS could inhibit inflammatory responses in lipopolysaccharide-induced endothelial cells, cigarette smoke extract-induced chronic obstructive pulmonary disease mice and hemorrhagic shock-induced rat models, via modulating mitogen-activated protein kinases (MAPKs)/nuclear factor kappa B (NF-κB) pathways [8–12]. In addition, STS is able to alleviate the disruption of cerebrovascular integrity by regulating the Rho-associated protein kinase (ROCK)-mediated cellular contractility in human umbilical vein endothelial cells and zebrafish models [10,13]. Interestingly, previous studies have reported that TIIA could alleviate tissue damages and provide anti-nociceptive effects in RA mice, which provides evidence supporting potential roles of STS in RA treatments [14–16]. However, protective actions of STS on RA-FLSs are still unveiled. Thus, in the current study, we aimed to investigate the effects of STS on inflammation, proliferation, migration, and invasion of human fibroblast-like synoviocytes rheumatoid arthritis (RA-HFLSs) and its underlying mechanisms [17]. Also, we investigated STS actions on collagen-induced arthritis (CIA) in mice in vivo [17].

* Corresponding author at: Department of Orthopedics, the First People's Hospital of Yunnan Province, No.157, Jinbi Road, Xishan District, 650000 Kunming, Yunnan, the People's Republic of China.
E-mail address: xiexuhua606@163.com (X. Xie).
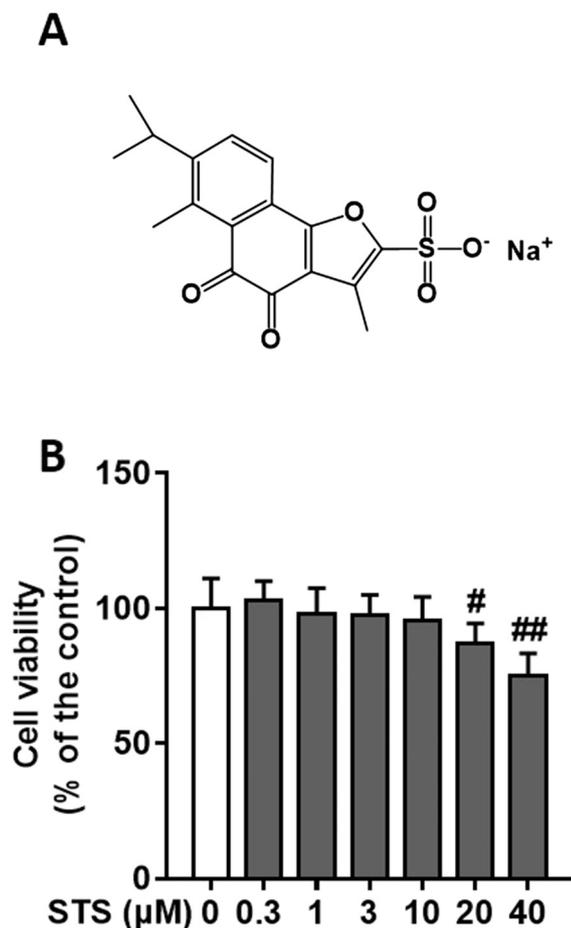
A

B

Fig. 1. Chemical structure of STS and STS effects on RA-HFLSs viability. (A) Chemical structure of STS was shown. (B) RA-HFLSs (1×10^4 cells) were treated with various doses of STS for 24 h, and cell viability was measured via CCK8 assay. The cell viability was expressed as % of the control. Results are showed as means ± SEM (n = 9). Control group was untreated cells. $^{\#}P < 0.05$ and $^{\#\#}P < 0.01$, versus control group.

2. Materials and methods

2.1. Chemical and reagents

Sodium tanshinone IIA sulfonate (STS, powers, purity: ≥98% HPLC-UV, the chemical structure was shown in Fig. 1A) was obtained from Chengdu Must Biotechnology Company (Chengdu, China). The STS was endotoxin-free. The DMEM and F-12K medium, fetal bovine serum were obtained from Gibco (Grand Island, NY, USA). TNF-α and BSA were obtained from Pepro Tech (Grand Island, NY, USA). The bovine type II collagen, Freund's complete adjuvant, and Freund's incomplete adjuvant were obtained from Sigma (St. Louis, MO, USA).

2.2. Cell culture and treatment

The RA-HFLSs was purchased from the ATCC (Manassas, VA, USA) and maintained in DMEM medium supplied with 10% FBS, 100 U/mL penicillin, and 100 mg/mL streptomycin with a humidified atmosphere 5% CO_2 at 37 °C. The RA-HFLSs that passage between 5 and 10 was used in this study. The experiment was conducted at 24 h after the RA-HFLSs were seeded. STS and other compounds were firstly dissolved in DMSO or H_2O as stock a solution and then was added into cell culture medium directly.

2.3. Experimental animal and protocol

Male DBA/1 mice (18–22 g, 8–9 weeks) were obtained from IMET Research Inc. (Nantong, China). The mice were maintained under SPF condition, with standard light-dark cycle, temperature, and humidity. All animal experiments were approved by the Institutional Animal Care, and Use Committee of the First People's Hospital of Yunnan Province (FPHYP-0029-2018) and all animals were treated in accordance with the National Institutes of Health Guide for the Care and Use of Laboratory Animals. Animals were randomly divided into to three groups (n = 10): Vehicle (normal animals were given normal saline), CIA (CIA animals were given normal saline), CIA + STS group (CIA animals given STS, 5 mg/kg, oral administrations, once a day, from day 21 to 48).

The CIA mice model was induced by twice immunization according to the protocol described in the previous study with small modifications [18–23]. In brief, DBA/1 mice were firstly given intradermal injections of bovine type II collagen emulsified in Freund's complete adjuvant (vol/vol, 1:1) as primary immunization on day 0, and then given secondary immunization using bovine type II collagen emulsified in incomplete Freund's adjuvant (vol/vol, 1:1) on day 21 [18–23]. The clinical symptoms and scores of limbs were collected and measured by two independent and blinded operators every three days from day 21 to day 48 [18–23]. The clinical arthritis score was assessed using a range of 0 to 4 (0, no change; 1, significant swelling and redness of one digit; 2, mild swelling and erythema of the limb or swelling of more than two digits; 3, marked swelling and erythema of the limb; 4, maximal swelling and redness of the limb and later, ankylosis), which was well described in previous studies [18–23]. On day 48, mice were euthanized using pentobarbital injections, and samples were obtained for the following studies [18–23].

2.4. Cell viability

Cell viability was detected using the Cell Counting Kit-8 (CCK-8) assay (Dojindo, Kumamoto, Japan) according to the manufacturer's protocols. In brief, RA-HFLSs were plated in the 96-wells cell culture plate and treated with different doses of STS (0, 1, 3, 10, 30 and 100 μM) for 24 h. Then, RA-HFLSs were incubated with CCK-8 reagents. Finally, the OD values (at 450 nm) were measured using a microplate reader.

2.5. Migration and invasion assay

The Boyden chamber methods were used to carry out the migration and invasion in RA-HFLSs [18–23]. The RA-HFLSs were planted in 24-wells plate with 6.5-mm diameter inserts containing 8-μm pores (Corning, Costar, NY, USA) [18–23]. For the migration assay, the RA-HFLSs were suspended in FBS-free DMEM and planted in upper chambers in the system. After that, 0.5 mL of medium supplied with 10% of FBS with or without STS (1, 3, and 10 μM) were added into lower chambers in the system. After 24 h, cells on upper surfaces of all filters were removed out using cotton swabs, and migratory cells that migrated into lower surfaces were fixed by paraformaldehyde about 10 min, stained by Hoechst 33342 for another 10 min, and finally imaged using a confocal laser-scanning microscope system (Olympus, Kyoto, Japan) at five independent visual fields.

For the invasion assay, RA-HFLSs cells were planted into upper chambers precoated with Matrigel reagents (BD Bioscience, CA, USA) in FBS-free DEME. 0.5 mL of medium supplied with 10% of FBS with or without STS (1, 3, and 10 μM) was added into lower chambers in the system. After 24 h, cells on upper surfaces of all filters were removed out using cotton swabs, and migratory cells that migrated into lower surfaces were fixed by paraformaldehyde about 10 min, stained by Hoechst 33342 for another 10 min, and finally imaged using a confocal laser-scanning microscope system at five independent visual fields.

2.6. Proliferation assays

The RA-HFLSs cells were firstly labeled by EdU (5-ethynyl-2′-deoxyuridine) using the BeyoClick™ EdU-488 cell proliferation assay kit (Beyotime, Shanghai, China). Then, RA-HFLSs cells were dissociated, counted, and seeded into plates and incubated with or without TNF-α (10 ng/mL) TNF or STS (0, 1, 3 and 10 μM) for 24 h. After that, cells were collected, washed and finally imaged using a confocallaser-scanning microscope system.

2.7. Immunofluorescence assay of the actin cytoskeleton

Cells were collected, washed, fixed in paraformaldehyde, permeabilized by Triton X-100 in PBS, and finally blocked with blocking buffers. After that, samples were incubated with primary antibodies for 12 h at 4 °C and Alexa-Fluor 488 or 596 secondary antibodies (1:500 dilutions, Invitrogen, CA, USA) for 0.5 h at room temperature, respectively. Cells were mounted with Prolong-anti-fade reagents and finally imaged a confocal-laser-scanning microscope system.

2.8. Enzyme-linked immunosorbent assay (Elisa)

RA-HFLSs cells were pretreated with various doses of STS for 1 h and then stimulated with TNF-α (10 ng/mL) for another 24 h. After that, the IL-6, IL-1β, MMP-1, and MMP-3 released into cells conditioned media, or supernatants of lysed tissues were measured using specific ELISA Ready SET Go Kits (eBiosciences, San Diego, CA, USA).

2.9. Quantitative PCR (qPCR) assay

Total RNA was extracted using TRIzol reagents (Invitrogen, Carlsbad, CA) following the manufacturer's protocols. The isolated RNA was reverse transcribed into prepared cDNA using the MMLV reverse transcriptase (Santa Cruz, CA, USA). The qPCR assay was performed using fast start universal SYBR-Green master reagents (Roche) with the ABI Prism 7500 real-time PCR system (Applied Biosystems, Foster City, CA, USA). The relative expression of each target gene compared with GAPDH was calculated using the comparative Ct method. The primer sequence used in the current study was listed in Table 1.

2.10. Western blot assay

The nuclear and cytoplasmic protein was prepared according to the manufacturer's protocols (Beyotime, Shanghai, China). The protein concentration was measured using the BCA™ Protein Assay kit (Invitrogen). Equal amounts of protein were subjected to SDS-PAGE, and then electrically transferred onto PVDF membranes (Bio-Rad, CA, USA). Subsequently, membranes were blocked for 1 h with 5% non-fat milk in TBS-0.1% Tween 20 (TBST), and incubated with primary antibodies: p-TAK-1, p-IKKα/β, t-IKKα, p-IκBα, t-IκBα, p-p65, t-p65, p-p38, t-p38, p-ERK1/2, t-ERK1/2, p-JNK, t-JNK, GAPDH and β-actin, and

Table 1
The primer sequences.

Name		Sequence (5′ to 3′)
IL-1β	F	GGCAACTGTTCCTGAACTCAACTG
	R	CCATTGAGGTGGAGAGCTTTCAGC
IL-6	F	AAGCCAGAGCTGTGCAGATGAGTA
	R	CTTGGTCACCGACGTCCTGT
MMP-1	F	CAGAGATGAAGTCCGGTTTTTC
	R	GGGGTATCCGTGTAGCACAT
MMP-3	F	CAAAACATATTTCTTTGTAGAGGACAA
	R	TTCAGCTATTTGCTTGGGAA
GAPDH	F	TGGAAGGACTCATGACCACA
	R	AGGGGTCTACATGGCAACTG

peroxidase-conjugated secondary antibodies for overnight at 4 °C and for 1 h at room temperature, respectively (CST, Danvers, MA, USA). Finally, protein bands were visualized using an ECL-plus-Western-blotting detection reagent (GE Healthcare, WI, USA). Images of bands were captured by the ChemiDoc XRS Molecular Imager and analyzed using the Bio-Rad Quantity-One Software (Bio-Rad).

2.11. Histochemical analysis

At the termination of the experiment, hind limbs with overlying skins from each animal were excised and fixed in 10% neutral-buffered-formalin solutions. Then, tissues were decalcified in 10% of EDTA and embedded in paraffin. The 4 μm thick section was made and stained with hematoxylin and eosin (H&E) kit for histological observations.

2.12. Graphing and statistical analysis

All data were present as mean means ± S.E.M. for at least three independent experiments. Data were analyzed by GraphPad Prism 6.0 (San Diego, CA, USA). Statistical significance was assessed by one-way or two-way ANOVA with Bonferroni's correction. $P < 0.05$ was considered significant in all analyses.

3. Results

3.1. Effect of STS on cell viability of RA-HFLSs

To investigate effects s of STS, we firstly measured STS potential cytotoxicity in RA-HFLSs using the CCK8 assay. As shown in Fig. 1B, no obvious cytotoxic effect was observed in RA-HFLSs exposed to 0 to 10 μM of STS for 24 h. Therefore, concentrations lower than 10 μM were used for the following experiments.

3.2. STS suppressed migration and invasion of RA-HFLSs

We then investigated the effects of STS on migration and invasion in RA-HFLSs using the trans-well Boyden chamber method. As shown in Fig. 2A, we found that STS could significantly decrease the migration RA-HFLSs, when compared with the control group (compared with the control group, $P < 0.01$). In addition, as shown in the invasion assay results, STS could also suppress the invasion of RA-HFLSs in a dose-dependent manner (Fig. 2B, $P < 0.01$).

3.3. STS suppressed proliferation in TNF-α-treated RA-HFLSs

RA-HFLSs proliferation plays a critical role in RA progress. Encouraged by the inhibitory actions of STS on migration and invasion, we here also detected the STS effects on proliferation in RA-HFLSs. As shown in Fig. 3, TNF-α could induce the RA-HFLSs proliferation (compared with the control group, all $P < 0.01$), however, STS treatment could dose-dependently suppress TNF-α-induced proliferation (compared with the TNF-α-treated group, all $P < 0.01$).

3.4. STS suppressed cytoskeleton alterations of TNF-α-induced RA-HFLSs

It is well known that dynamic reorganizations of actin cytoskeleton contribute to migration and invasion in RA-HFLSs. To confirm the STS actions on RA-HFLSs, we then performed the immunofluorescence staining to visualize the affection on F-actin reorganization. As reported in previous reports, in our study, we also found that TNF-α (10 ng/mL) could significantly increase actin stress fiber formation (data were shown in Fig. 4). However, STS treatment was able to reduce the intensity of F-actin stress fibers in TNF-α-treated RA-HFLSs.
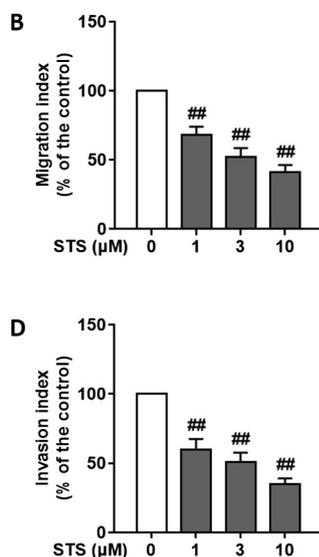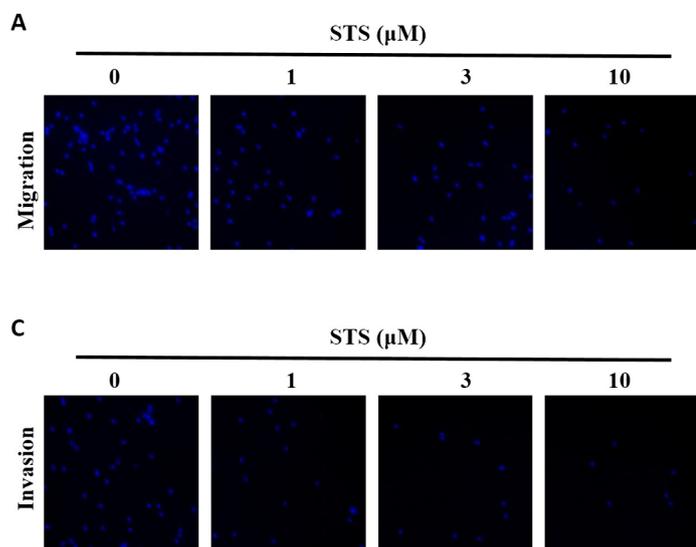
A

B

C

D

Fig. 2. Effect of STS on migration and invasion of RA-HFLSs.

(A) RA-HFLSs (1×10^4 cells) were treated with various doses of STS for 24 h, and then migration was tested using a Boyden trans-well chamber, and chemotaxis was quantified by counting the migration index (% of the control), scale bar: $200\times$. (B) Cell invasion was determined using a Matrigel basement membrane matrix chamber, and the invading cells were quantified by counting the invasion index (% of the control), scale bar: $200\times$. Results are showed as means ± SEM (n = 9). Control group was untreated cells. $^{\#}P < 0.05$ and $^{\#\#}P < 0.01$, versus control group.

3.5. STS repressed MMPs production in RA-HFLSs exposed to TNF-α

MMPs play an important role in the RA progression. Therefore, we then detected the actions of STS on MMPs productions in TNF-α-treated RA-HFLSs. As demonstrated in Fig. 5A and B, when compared to the control cells, TNF-α (10 ng/mL) could obviously increase the mRNA level of MMP-1 and MMP-3 in RA-HFLSs (all $P < 0.01$). However, STS treatment inhibited the mRNA expression of MMP-1 and MMP-3 in TNF-α-treated RA-HFLSs (compared with the TNF-α-treated group, all $P < 0.01$). Moreover, STS could significantly down-regulate the protein level of MMP-1 and MMP-1 in TNF-α-induced RA-HFLSs (Fig. 5C and D, compared with the TNF-α-treated group, all $P < 0.01$).

3.6. STS decreased pro-inflammatory cytokines production in RA-HFLSs exposed to TNF-α

Overproduction of pro-inflammatory cytokines, including IL-6 and IL-1B in RA-HFLSs, was reported to be well involved in the pathogenesis of RA. Here, we also detect the possible inhibitory role of STS against the production of pro-inflammatory cytokines in TNF-α-treated RA-HFLSs. As shown in Fig. 6A and B, TNF-α (10 ng/mL) significantly increased the mRNA expression of IL-6 and IL-1β in RA-HFLSs (compared with the control group, all $P < 0.01$). However, STS treatment inhibited the increase of IL-6 and IL-1B mRNA expression in TNF-α-treated RA-HFLSs (compared with the TNF-α-treated group, all $P < 0.01$). Moreover, STS also significantly down-regulated the protein level of IL-6 and IL-1β in TNF-α-induced RA-HFLSs (Fig. 6C and D, compared with the TNF-α-treated group, all $P < 0.01$).

3.7. STS inhibited MAPKs and NF-κB activations in TNF-α-induced RA-HFLSs

MAPK signaling pathways are crucial for RA-FLSs migration, proliferation, and inflammatory cytokine expression. And NF-κB is an important modulator of the inflammatory process in the development of RA. To further explore the underlying mechanisms of STS in cell proliferation, migration, invasion, and inflammatory response; we then examined actions of STS on MAPKs and NF-κB pathways in TNF-α-induced RA-HFLSs.

Firstly, as shown in Fig. 7, the level of phosphorylated p38, JNK and ERK were significantly increased in cells exposed to TNF-α (compared with the control group, all $P < 0.01$). However, STS treatment (3 and 10 μM) could significantly suppress the TNF-α-induced phosphorylation of p38, JNK and ERK in RA-HFLSs (compared with the TNF-α-treated group, all $P < 0.01$).

Next, as shown in Fig. 8, we also found that STS could also decrease TNF-α-induced phosphorylation of NF-κB p65 and IκBα (compared with the TNF-α-treated group, all $P < 0.01$). Moreover, STS treatment could significantly inhibit TNF-α-induced degradation of IκBα in RA-HFLSs (Fig. 8, compared with the TNF-α-treated group, all $P < 0.01$). Normally, NF-κB was activated by TAK1 via regulating interactions with TNF receptor-associated factor (TRAF)-6. The level of TAK1 phosphorylation was also detected in this study. The results demonstrated that STS (10 μM) significantly decreased the level of phosphorylated-TAK1 in RA-HFLSs (Fig. 8, compared with the TNF-α-treated group, all $P < 0.01$).
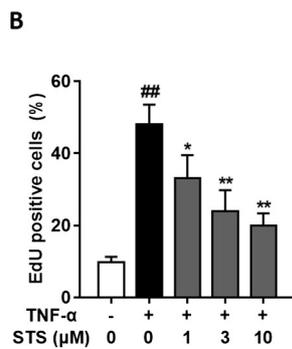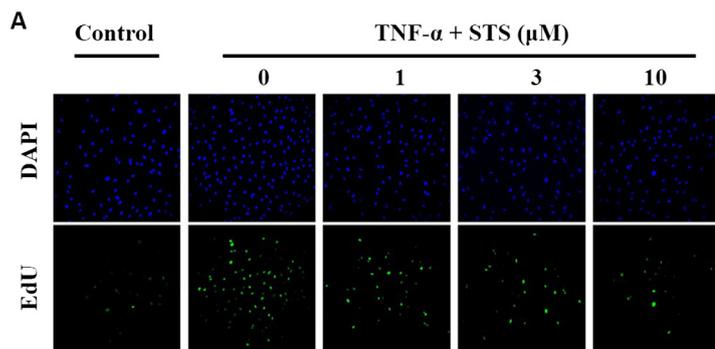
A

B

Fig. 3. Effect of STS on TNF-α-induced proliferation in RA-HFLSs.

(A) The EdU cell proliferation assay was used to assess cell proliferation in RA-HFLSs (1×10^4 cells) after treatment with STS or TNF-α (10 ng/mL) for 24 h. (B) And then EdU positive cells ratio were quantified by counting the number of positive cells to total cells (%), scale bar: $100\times$. Results are showed as means ± SEM (n = 9). Control group was untreated cells. $^{\#}P < 0.05$ and $^{\#\#}P < 0.01$, versus control group. $^{*}P < 0.05$ and $^{**}P < 0.01$, versus TNF-α-treated group.
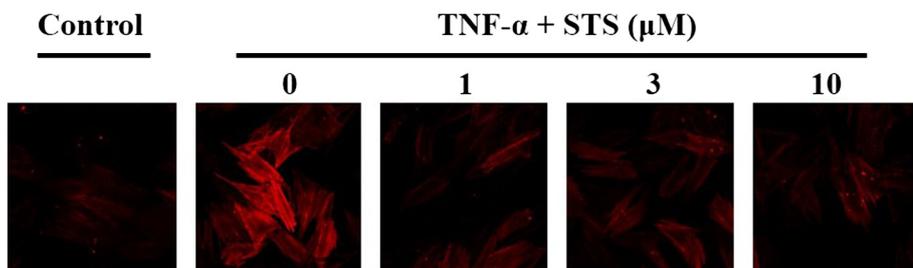
Fig. 4. Effect of STS on TNF-α-induced cytoskeletal reorganization in RA-HFLSs.
The RA-HFLSs (1×10^4 cells) were treated with or without STS or TNF-α (10 ng/mL) for 24 h. And then cells were fixed and stained with fluorescent phalloidin and DAPI to visible F-actin (red) and nuclei (blue). Representative images from three independent experiments are shown here (n = 9); scale bar: 400×. Control group was untreated cells. (For interpretation of the references to colour in this figure legend, the reader is referred to the web version of this article.)

3.8. STS alleviated arthritis progression and damages in CIA mice

To further investigate potential therapeutic actions of STS on RA in vivo, the CIA-induced RA mice model was performed in our study. We found that STS treatment could significantly decrease clinical arthritis scores in CIA mice (Fig. 9A, compared with the vehicle-treated group, all $P < 0.01$). Moreover, the histopathological analysis also showed STS treatments could alleviate inflammatory infiltration, synovial hyperplasia, and cartilage destruction in joints tissue of CIA mice (shown in Fig. 9B).

4. Discussion

Previous studies have provided evidence supporting the potential protective actions of STS in RA [8–12]. In the present study, we demonstrated that STS could suppress the migration and invasion and inflammation in human fibroblast-like synoviocytes rheumatoid arthritis (RA-HFLSs). Then, we also demonstrated that STS treatment could attenuate synovial inflammation and joint destruction in collagen-induced arthritis (CIA) mice. Moreover, we found that STS could

block TNF-α-induced MAPKs and NF-κB activation in RA-HFLSs. Thus, our findings suggested that STS conferred inhibitory effects on aggressive behaviors of RA-HFLSs by blocking MAPKs and NF-κB activations, which might be developed as novel agents for RA treatments.

Accumulating evidence indicates that the activated RA-FLSs display tumor cells-like biological characteristics, like aggressive proliferation, migration, and invasion, which contributes to damages of cartilage, joint and bone [6,7,24]. Firstly, it is well reported that abnormal proliferation of RA-FLSs contribute to synovial hyperplasia [6,7,24]. Usually, RA-FLSs locate at the joint surface, destroy cartilage and activate osteoclasts, resulting in bone erosion and destruction [6,7,24]. Therefore, migration and invasion of RA-FLSs into cartilages is also well associated with the joint destruction in RA [6,7,24]. Thus, modulating RA-FLSs proliferation, migration and invasion are supported to be novel therapeutic strategies for preventing destructive progress in RA [19–23]. In agreement with the previous reports that STS could suppress the proliferation and migration of endothelial cells [8–12], in the current study, we also confirmed inhibitory effects of STS on proliferation, migration, and invasion of RA-HFLSs. It is well known that cells cytoskeleton rearrangements participate in regulating the
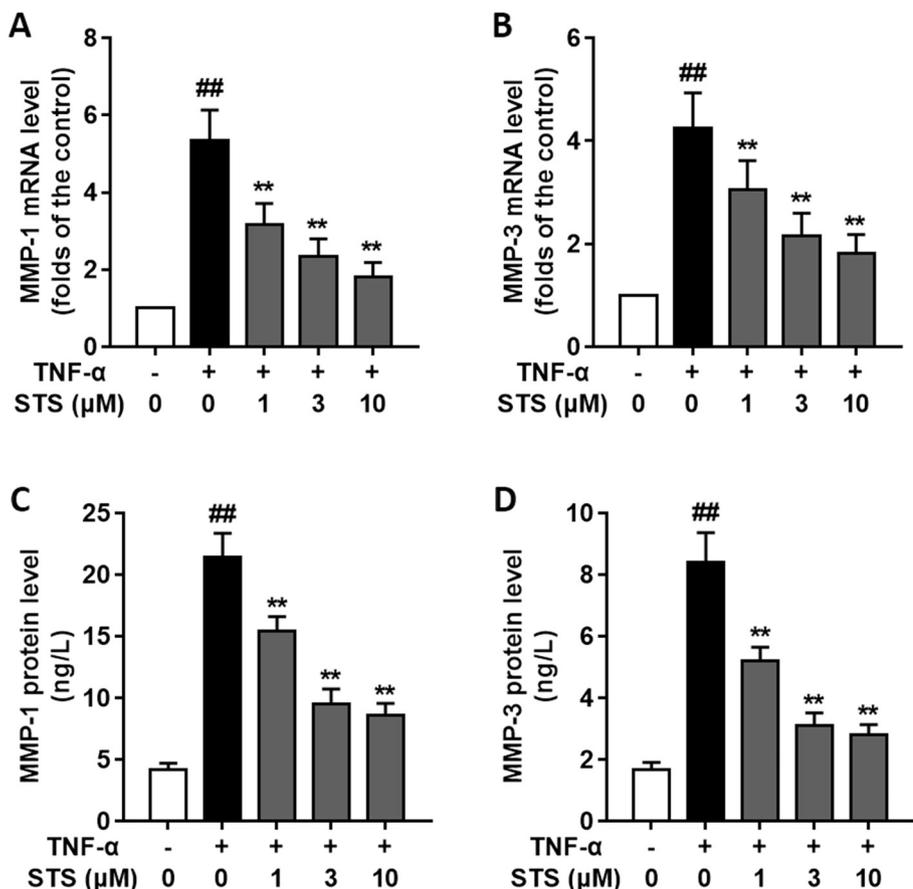

Fig. 5. Effect of STS on TNF-α-induced MMPs production in RA-HFLSs.
The RA-HFLSs (1×10^4 cells) were treated with or without STS or TNF-α (10 ng/mL) for 24 h. (A and B) After that, the total mRNA was extracted, and the mRNA expression of MMP-1 and MMP-3 were analyzed using qPCR. The mRNA level was normalized to GAPDH and expressed as folds of the control group. (C and D) The protein was prepared, and the protein level of MMP-1 and MMP-3 were detected using Elisa. Results are showed as means ± SEM (n = 9). Control group was untreated cells. $^{\#}P < 0.05$ and $^{\#\#}P < 0.01$, versus control group. $^{*}P < 0.05$ and $^{**}P < 0.01$, versus TNF-α-treated group.
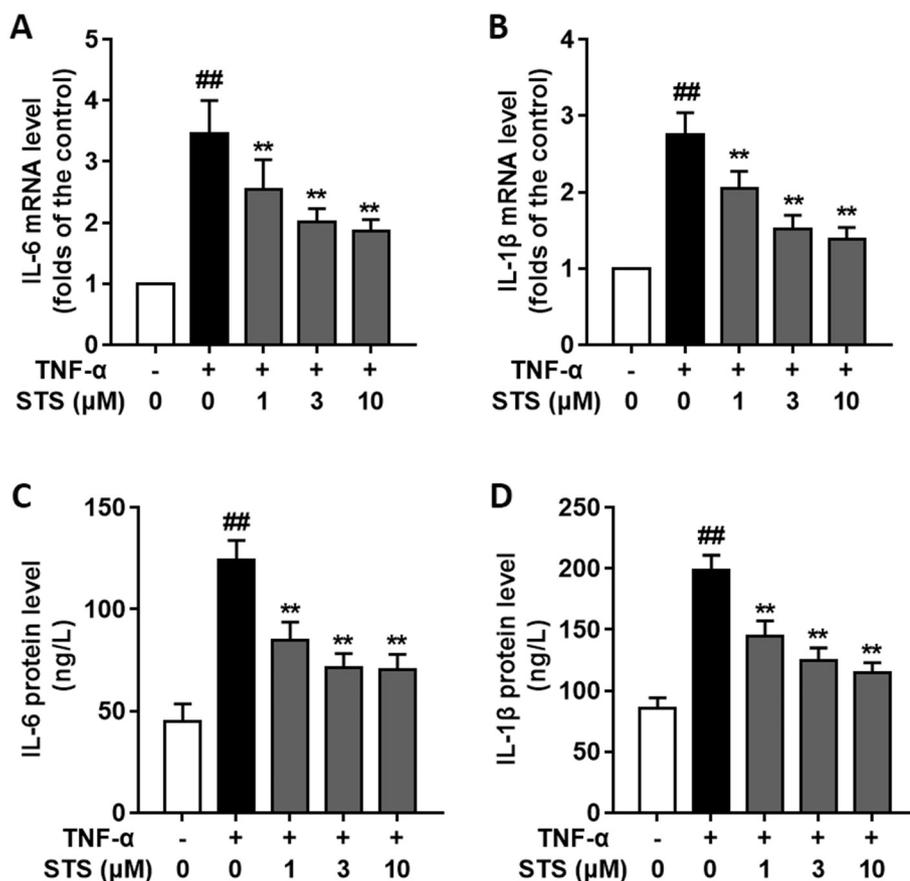
Fig. 6. Effect of STS on TNF-α-induced IL-6, IL-1β production in RA-HFLSs.

The RA-HFLSs (1×10^4 cells) were treated with or without STS or TNF-α (10 ng/mL) for 24 h. (A and B) After that, the total mRNA was extracted, and the mRNA expression of IL-6 and IL-1β were analyzed using qPCR. The mRNA level was normalized to GAPDH and expressed as fold of the control group. (C and D) The protein was prepared, and the protein level of IL-6 and IL-1β were detected using Elisa. Results are showed as means ± SEM (n = 9). Control group was untreated cells. $^{\#}P < 0.05$ and $^{\#\#}P < 0.01$, versus control group. $^{*}P < 0.05$ and $^{**}P < 0.01$, versus TNF-α-treated group.

direction of cell migration and invasion, which is a tightly coordinated process [19,25,26]. Here, we also found that STS could prevent cytoskeletal reorganization in RA-HFLSs as evidenced by inhibition on F-actin remodeling in TNF-α-stimulated cells, which are key steps that control cells migration and invasion, further supporting ours in vitro findings. In conclusion, we demonstrated that STS could suppress proliferation, migration, and invasion of RA-FLSs. These findings suggested

STS might be beneficial for the prevention of joint destruction in treatments.

The RA-FLSs play an important role in RA development, which are well associated with inflammatory response, synovial hyperplasia, joint destruction, and various kinds of comorbidity [1–5]. The inflammatory cytokines, especially IL-6 and IL-1β, play a key role in synovial inflammation in the RA process [27–29]. Increasing evidence suggests
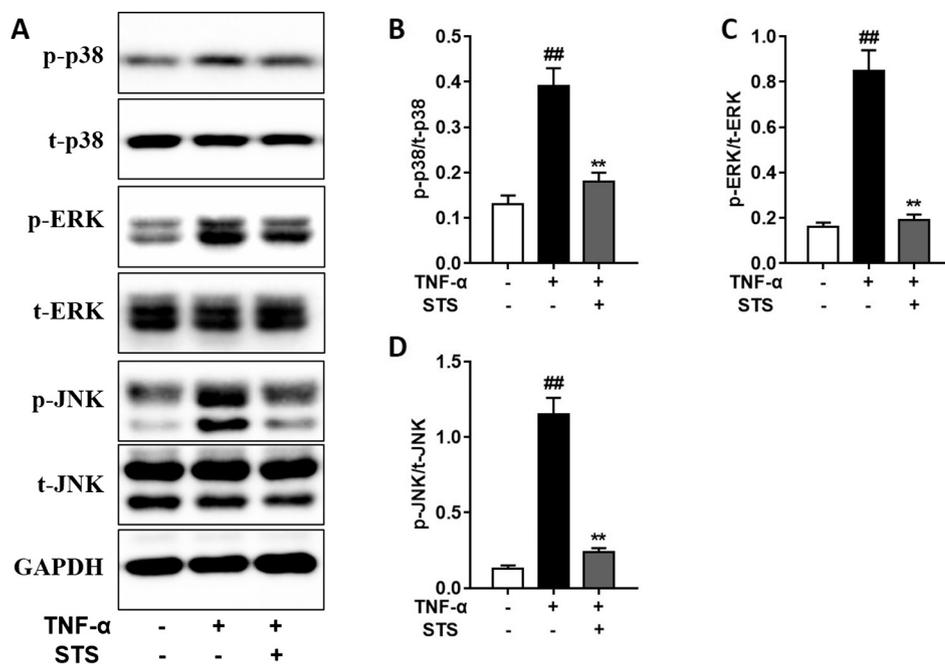

Fig. 7. Effect of STS on MAPKs pathways in TNF-α-induced RA-HFLSs.

The RA-HFLSs (1×10^4 cells) were treated with or without STS or TNF-α (10 ng/mL). After that, the protein was prepared and the level of phosphorylated and total p38, JNK and ERK protein was detected by Western blot. Results are showed as means ± SEM (n = 5). Control group was untreated cells. $^{\#}P < 0.05$ and $^{\#\#}P < 0.01$, versus control group. $^{*}P < 0.05$ and $^{**}P < 0.01$, versus TNF-α-treated group.
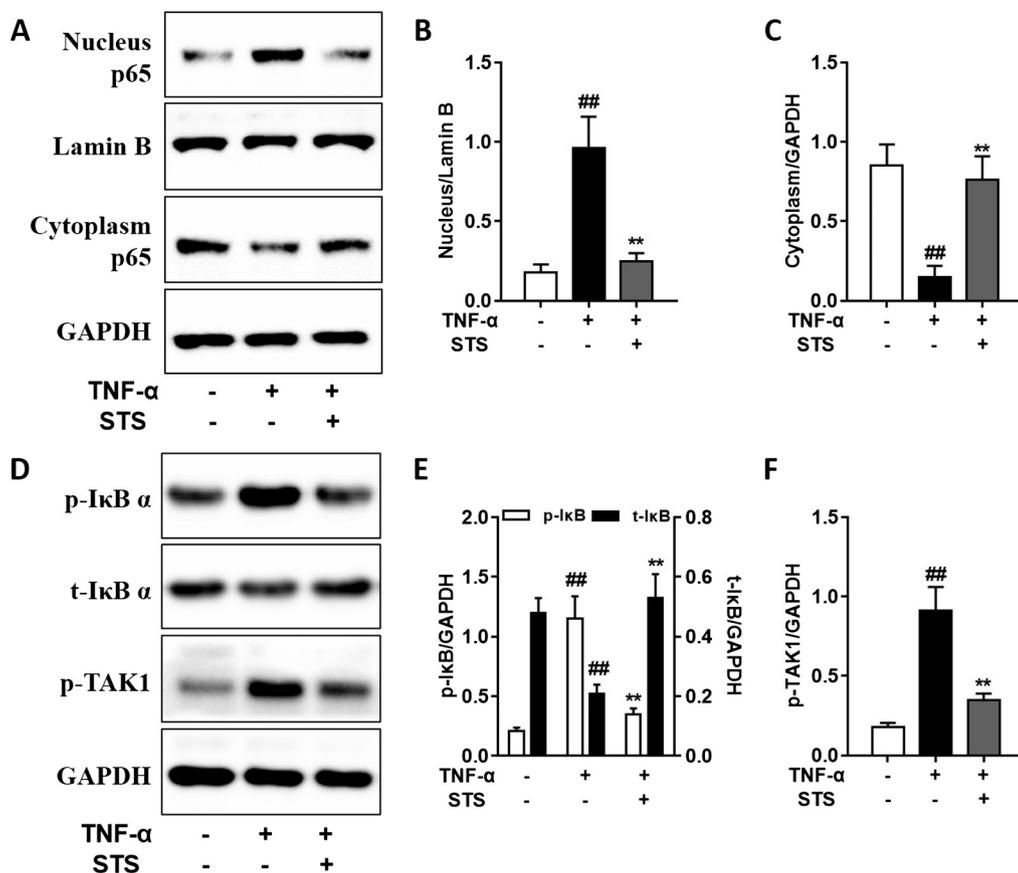
Fig. 8. Effect of STS on NF-κB pathways in TNF-α-induced RA-HFLSs.

The RA-HFLSs (1×10^4 cells) were treated with or without STS or TNF-α (10 ng/mL). After that, the protein was prepared, and the level of phosphorylated and total p65 and IκBα protein was detected by Western blot. Results are showed as means ± SEM (n = 5). Control group was untreated cells. $^\#P < 0.05$ and $^{\#\#}P < 0.01$, versus control group. $^*P < 0.05$ and $^{**}P < 0.01$, versus TNF-α-treated group.
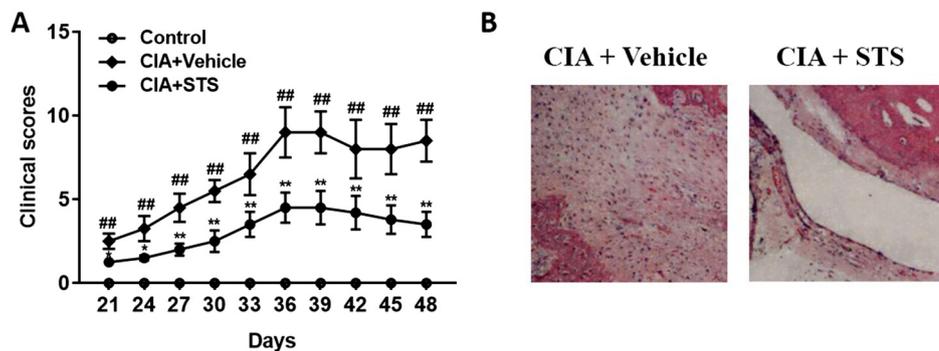

Fig. 9. Effects of STS on arthritis progression and alleviated synovial inflammation in CIA mice.

CIA was induced by two times of immunization in mice. Animals were administrated with vehicle or STS (10 mg/kg) on every other day from day 0 to day 48. Clinical symptoms and score of limbs were observed and recorded from day 21. On day 48, animals were sacrificed, and synovial tissues were collected. (A) Effects of STS on arthritis scores in CIA mice. (B) Representative histological assessment of joint in CIA mice on day 48 (400×). Results are showed as means ± SEM (n = 5). $^\#P < 0.05$ and $^{\#\#}P < 0.01$, versus control group; $^*P < 0.05$ and $^{**}P < 0.01$, versus the vehicle-treated group.

that activated RA-FLSs could produce and secrete inflammatory cytokines that deteriorate the RA progression [1–5]. Thus, the discovery of anti-inflammatory agents is considered as one of the important strategies for RA treatments [27–29]. Accumulating evidence indicates that inhibitory effects against inflammation and oxidative stress by STS contribute to its protections on cardiovascular diseases. Previous studies have demonstrated that STS could inhibit inflammatory responses in lipopolysaccharide-induced endothelial cells [8–12]. It has been widely reported TNF-α induces activation of RA-HFLSs and trigger the production of inflammatory cytokine and mediator [27–29]. As a first step towards the application of STS, we detected STS effects on proinflammatory cytokines in TNF-α-stimulated RA-HFLSs. In our study, we also confirmed that STS could suppress expressions of IL-1β and IL-6 in TNF-α-stimulated RA-HFLSs.

MMPs, the major proteases involved in the invasion and degradation of anatomical barriers, have a role in extracellular matrix degradation [7]. The TNF-α treatment has been well reported to induce MMPs expressions in RA-FLSs, and these processes are mainly regulated by transcriptional and translational levels [30,31]. Among MMPs, MMP-1 and MMP-3are markedly elevated in synovial fluid from RA patients and collagen degradation, causing disease progression and bone erosion [32–34]. MMPs expressions could be induced by pro-inflammatory cytokines, like TNF-α in RA-FLSs. And previous reports also indicate that MMPs are down-regulated in response to the anti-TNF therapy [32,33]. It is well reported that MMP expression is well associated with FLS migration and invasion in RA-FLSs [32,33]. In our study, TNF-α induced increasing production of both MMP-1 and MMP-3 in RA-HFLSs. In the present study, we observed that STS treatment markedly down-regulated the TNF-α-induced production of MMP-1 and MMP-3 in RA-HFLSs, suggesting that one of the mechanisms for STS-regulated aggressive behavior of RA FLSs is reducing MMP-1 and MMP-3 production.

Increasing evidence demonstrates that MAPKs, including p38, ERK, and JNK, not only play an important role in the inflammatory response in RA-FLSs but also participate in the migration, invasion, actin cytoskeletal reorganization in RA-FLSs [35–37]. Discovery of drugs that

targeting MAPK pathways is supported to be therapeutic strategies for preventing RA progress [19–23]. Previous studies have demonstrated that STS could inhibit inflammatory responses in various models, via modulating MAPKs pathways [8–12]. Thus, in the current study, we also investigate STS effects on MAPK pathways in RA-HFLSs. In accord with previous studies, we found that TNF-α stimulation could induce activation of p38, ERK, and JNK in RA-FLSs [19–23]. In the current study, we observed that STS could block the activation of MAPKs, as evidenced by inhibiting phosphorylation of p38, ERK, and JNK. Notedly, several compounds, including triptolide, kaempferol, oxymatrine, and betulinic acid have been reported to suppress migration and invasion in RA-FLSs via modulating MAPKs pathways [19–23]. Thus, we suggested that inhabiting MAPKs activation in TNF-α-stimulated RA-FLSs might be potential mechanisms for STS-mediated suppression of proliferation, migration, invasion, actin cytoskeletal reorganization.

It is well reported that NF-κB pathways well participate in regulating inflammation in RA-FLSs [38–43]. Inhibiting NF-κB activity has been considered an important target for controlling synovial inflammation, synovial hyperplasia, and matrix degenerations [38–43]. Previous studies have demonstrated that STS could inhibit inflammatory responses in various models, via modulating NF-κB pathways [8–12]. Therefore, we here postulated that STS could suppress NF-κB activation in RA-HFLSs [19–23]. Our results demonstrated that STS could inhibit phosphorylation of NF-κB and IκBα, and suppress degradation of IκBα protein. Current data also confirmed that STS could block the NF-κB nuclear accumulation induced by TNF-α. Usually, NF-κB pathways are modulated by TAK1 via regulating TRAF-6 [38–40]. In this study, we also confirmed that STS modulated the phosphorylation of TAK1, suggesting that TAK1 should be one of the upstream modulators of NF-κB mediated by STS [38–40]. These findings suggested that STS provide protective effects against RA by blocking NF-κB activation via regulating TAK1 and IκB pathways.

The CIA-induced RA models are the most common models of RA and CIA has been widely used in different kinds of studies to investigate RA pathogenesis and discovery agents for RA treatments [19–23,44–48]. To further detect the effects of STS against RA, CIA-induced RA mice was also performed in our study. Treatments of RA mice with STS could significantly decrease clinical scores and alleviate synovial inflammation. Due to several limitations, we did not conduce experiments to detect the accumulating content of STS in the joints of RA mice. Since that it is important to exclude that the effects of STS in vivo are simply indirect effects, we would perform the pharmacokinetics and tissue distribution study of STS in mice. In summary, this study provided evidence to support the notion that STS conferred therapeutic effects on RA progression and inflammatory damage in mice.

In conclusion, this study provided evidence that STS inhibited proliferation, migration, invasion, and inflammation in RA-HFLSs and attenuated RA progression in CIA mice. Our findings suggested that inhibition of MAPKs and NF-κB pathways might contribute to STS-mediated inhibitory actions against RA. These results demonstrated that STS might be developed as novel agents for RA treatments.

Declaration of Competing Interest

The authors have declared no conflicts of interest.

Acknowledgments

References

[1] S. Lefevre, A. Knedla, C. Tennie, A. Kampmann, C. Wunrau, R. Dinser, A. Korb, E.M. Schnaker, I.H. Tarner, P.D. Robbins, C.H. Evans, H. Sturz, J. Steinmeyer, S. Gay, J. Scholmerich, T. Pap, U. Muller-Ladner, E. Neumann, Synovial fibroblasts spread rheumatoid arthritis to unaffected joints, Nat. Med. 15 (12) (2009)

[2] L.C. Huber, O. Distler, I. Tarner, R.E. Gay, S. Gay, T. Pap, Synovial fibroblasts: key players in rheumatoid arthritis, Rheumatology 45 (6) (2006) 669–675.

[3] K.F. Zhai, H. Duan, L. Luo, W.G. Cao, F.K. Han, L.L. Shan, X.M. Fang, Protective effects of paeonol on inflammatory response in IL-1 beta-induced human fibroblast-like synoviocytes and rheumatoid arthritis progression via modulating NF-kappa B pathway, Inflammopharmacology 25 (5) (2017) 523–532.

[4] N. Bottini, G.S. Firestein, Duality of fibroblast-like synoviocytes in RA: passive responders and imprinted aggressors, Nat. Rev. Rheumatol. 9 (1) (2013) 24–33.

[5] B. Bartok, G.S. Firestein, Fibroblast-like synoviocytes: key effector cells in rheumatoid arthritis, Immunol. Rev. 233 (2010) 233–255.

[6] Y. Dai, J. Ding, W. Yin, Y. He, F. Yu, C. Ye, S. Hu, Y. Yu, Increased autophagy enhances the resistance to tumor necrosis factor-alpha treatment in rheumatoid arthritis human fibroblast-like synovial cell, Biomed. Res. Int. 2018 (2018) 4941027.

[7] A. Mor, S.B. Abramson, M.H. Pillinger, The fibroblast-like synovial cell in rheumatoid arthritis: a key player in inflammation and joint destruction, Clin. Immunol. 115 (2) (2005) 118–128.

[8] D.F. Li, J. Wang, D.J. Sun, X.F. Gong, H. Jiang, J.Z. Shu, Z.Y. Wang, Z. Long, Y.G. Chen, Z.L. Zhang, L. Yuan, R.J. Guan, X. Liang, Z.Y. Li, H.W. Yao, N.S. Zhong, W.J. Lu, Tanshinone IIA sulfonate protects against cigarette smoke-induced COPD and down-regulation of CFTR in mice, Sci. Rep. 8 (2018).

[9] Q.H. Hu, B. Wei, L.L. Wei, K. Hua, X. Yu, H.Q. Li, H. Ji, Sodium tanshinone IIA sulfonate ameliorates ischemia-induced myocardial inflammation and lipid accumulation in Beagle dogs through NLRP3 inflammasome, Int. J. Cardiol. 196 (2015) 183–192.

[10] J. Cheng, T.T. Chen, P.Y. Li, J. Wen, N.B. Pang, L.P. Zhang, L.Q. Wang, Sodium tanshinone IIA sulfonate prevents lipopolysaccharide-induced inflammation via suppressing nuclear factor-kappa B signaling pathway in human umbilical vein endothelial cells, Can. J. Physiol. Pharmacol. 96 (1) (2018) 26–31.

[11] C. Qian, Y. Ren, Y.S. Xia, Sodium tanshinone IIA sulfonate attenuates hemorrhagic shock-induced organ damages by nuclear factor-kappa B pathway, J. Surg. Res. 209 (2017) 145–152.

[12] R.F. Yang, A.J. Liu, X.J. Ma, L. Li, D.F. Su, J.G. Liu, Sodium tanshinone IIA sulfonate protects cardiomyocytes against oxidative stress-mediated apoptosis through inhibiting JNK activation, J. Cardiovasc. Pharmacol. 51 (4) (2008) 396–401.

[13] Z.Y. Zhou, B. Huang, S. Li, X.H. Huang, J.Y. Tang, Y.W. Kwan, P.M. Hoi, S.M.Y. Lee, Sodium tanshinone IIA sulfonate promotes endothelial integrity via regulating VE-cadherin dynamics and RhoA/ROCK-mediated cellular contractility and prevents atorvastatin-induced intracerebral hemorrhage in zebrafish, Toxicol. Appl. Pharmacol. 350 (2018) 32–42.

[14] G. Li, Y. Liu, F. Meng, Z. Xia, X. Wu, Y. Fang, C. Zhang, D. Liu, Tanshinone IIA promotes the apoptosis of fibroblast-like synoviocytes in rheumatoid arthritis by up-regulating lncRNA GAS5, Biosci. Rep. 38 (5) (2018).

[15] S. Zhang, G. Huang, K. Yuan, Q. Zhu, H. Sheng, R. Yu, G. Luo, A. Xu, Tanshinone IIA ameliorates chronic arthritis in mice by modulating neutrophil activities, Clin. Exp. Immunol. 190 (1) (2017) 29–39.

[16] L. Jie, H. Du, Q. Huang, S. Wei, R. Huang, W. Sun, Tanshinone IIA induces apoptosis in fibroblast-like synoviocytes in rheumatoid arthritis via blockade of the cell cycle in the G2/M phase and a mitochondrial pathway, Biol. Pharm. Bull. 37 (8) (2014) 1366–1372.

[17] C. Liu, X. Kong, X. Li, W. Guo, C. Zhang, Y. Sun, X. Su, X. Liu, A. Lu, N. Lin, Wen Luo Yin inhibits angiogenesis in collagen-induced arthritis rat model and in vitro, J. Ethnopharmacol. 149 (2) (2013) 478–489.

[18] D.D. Brand, K.A. Latham, E.F. Rosloniec, Collagen-induced arthritis, Nat. Protoc. 2 (5) (2007) 1269–1275.

[19] J. Wang, Q. Zhao, Betulinic acid inhibits cell proliferation, migration, and inflammatory response in rheumatoid arthritis fibroblast-like synoviocytes, J. Cell. Biochem. 120 (2) (2019) 2151–2158.

[20] D.M. Pan, N. Li, Y.Y. Liu, Q. Xu, Q.P. Liu, Y.T. You, Z.Q. Wei, Y.B. Jiang, M.Y. Liu, T.F. Guo, X.D. Cai, X.B. Liu, Q. Wang, M.L. Liu, X.J. Lei, M.Y. Zhang, X.S. Zhao, C.S. Lin, Kaempferol inhibits the migration and invasion of rheumatoid arthritis fibroblast-like synoviocytes by blocking activation of the MAPK pathway, Int. Immunopharmacol. 55 (2018) 174–182.

[21] J. Liang, B.Y. Chang, M.C. Huang, W.C. Huang, W.K. Ma, Y. Liu, W. Tai, Y. Long, Y. Lu, Oxymatrine prevents synovial inflammation and migration via blocking NF-kappa B activation in rheumatoid fibroblast-like synoviocytes, Int. Immunopharmacol. 55 (2018) 105–111.

[22] J. Zuo, Q. Yin, Y.W. Wang, Y. Li, L.M. Lu, Z.G. Xiao, G.D. Wang, J.J. Luan, Inhibition of NF-kappa B pathway in fibroblast-like synoviocytes by alpha-mangostin implicated in protective effects on joints in rats suffering from adjuvant-induced arthritis, Int. Immunopharmacol. 56 (2018) 78–89.

[23] Y.L. Yang, Y.J. Ye, Q. Qiu, Y.J. Xiao, M.C. Huang, M.H. Shi, L.Q. Liang, X.Y. Yang, H.S. Xu, Triptolide inhibits the migration and invasion of rheumatoid fibroblast-like synoviocytes by blocking the activation of the JNK MAPK pathway, Int. Immunopharmacol. 41 (2016) 8–16.

[24] M.F. Bustamante, et al., Fibroblast-like synoviocyte metabolism in the pathogenesis of rheumatoid arthritis, Arthritis Res. Ther. 19 (2017) 110.

[25] M. Verderame, D. Alcorta, M. Egnor, K. Smith, P. Pollack, Cytoskeletal F-actin patterns quantitated with fluorescein isothiocyanate-phalloidin in normal and transformed cells, Proc. Natl. Acad. Sci. U. S. A. 77 (11) (1980) 6624–6628.

[26] J.Y. Lee, et al., Anti-inflammatory effects of ursolic acid-3-acetate on human synovial fibroblasts and a murine model of rheumatoid arthritis, Int. Immunopharmacol. 49 (2017) 118–125.

[27] M.C. Boissier, Cell and cytokine imbalances in rheumatoid synovitis, Joint Bone Spine 78 (3) (2011) 230–234.

[28] L.A. Joosten, M.M. Helsen, T. Saxne, F.A. van De Loo, D. Heinegard, W.B. van Den Berg, IL-1 alpha beta blockade prevents cartilage and bone destruction in murine type II collagen-induced arthritis, whereas TNF-alpha blockade only ameliorates joint inflammation, J. Immunol. 163 (9) (1999) 5049–5055.

[29] H. Kokkonen, I. Soderstrom, J. Rocklov, G. Hallmans, K. Lejon, S. Rantapaa Dahlqvist, Up-regulation of cytokines and chemokines predates the onset of rheumatoid arthritis, Arthritis Rheum. 62 (2) (2010) 383–391.

[30] T.C. Tolboom, E. Pieterman, W.H. van der Laan, R.E. Toes, A.L. Huidekoper, R.G. Nelissen, F.C. Breedveld, T.W. Huizinga, Invasive properties of fibroblast-like synoviocytes: correlation with growth characteristics and expression of MMP-1, MMP-3, and MMP-10, Ann. Rheum. Dis. 61 (11) (2002) 975–980.

[31] Y. Ou, W. Li, X. Li, Z. Lin, M. Li, Sinomenine reduces invasion and migration ability in fibroblast-like synoviocytes cells co-cultured with activated human monocytic THP-1 cells by inhibiting the expression of MMP-2, MMP-9, CD147, Rheumatol. Int. 31 (11) (2011) 1479–1485.

[32] M. Bjorklund, E. Koivunen, Gelatinase-mediated migration and invasion of cancer cells, Biochim. Biophys. Acta 1755 (1) (2005) 37–69.

[33] V.J. Richardson, Divergent and synergistic regulation of matrix metalloprotease production by cytokines in combination with C-C chemokines, Int. J. Immunopathol. Pharmacol. 23 (3) (2010) 715–726.

[34] X.N. Jin, E.Z. Yan, H.M. Wang, H.J. Sui, Z. Liu, W. Gao, Y. Jin, Hyperoside exerts anti-inflammatory and anti-arthritic effects in LPS-stimulated human fibroblast-like synoviocytes in vitro and in mice with collagen-induced arthritis, Acta Pharmacol. Sin. 37 (5) (2016) 674–686.

[35] F. Liu, X.X. Feng, S.L. Zhu, H.Y. Huang, Y.D. Chen, Y.F. Pan, R.R. June, S.G. Zheng, J.L. Huang, Sonic Hedgehog signaling pathway mediates proliferation and migration of fibroblast-like synoviocytes in rheumatoid arthritis via MAPK/ERK signaling pathway, Front. Immunol. 9 (2018) 2847.

[36] S.S. Nah, H.J. Won, E. Ha, I. Kang, H.Y. Cho, S.J. Hur, S.H. Lee, H.H. Baik, Epidermal growth factor increases prostaglandin E2 production via ERK1/2 MAPK and NF-kappaB pathway in fibroblast like synoviocytes from patients with rheumatoid arthritis, Rheumatol. Int. 30 (4) (2010) 443–449.

[37] J.E. Ha, Y.E. Choi, J. Jang, C.H. Yoon, H.Y. Kim, Y.S. Bae, FLIP and MAPK play crucial roles in the MLN51-mediated hyperproliferation of fibroblast-like synoviocytes in the pathogenesis of rheumatoid arthritis, FEBS J. 275 (14) (2008) 3546–3555.

[38] P. di Meglio, A. Ianaro, S. Ghosh, Amelioration of acute inflammation by systemic administration of a cell-permeable peptide inhibitor of NF-kappaB activation, Arthritis Rheum. 52 (3) (2005) 951–958.

[39] V.J. Palombella, E.M. Conner, J.W. Fuseler, A. Destree, J.M. Davis, F.S. Laroux, R.E. Wolf, J. Huang, S. Brand, P.J. Elliott, D. Lazarus, T. McCormack, L. Parent, R. Stein, J. Adams, M.B. Grisham, Role of the proteasome and NF-kappaB in streptococcal cell wall-induced polyarthritis, Proc. Natl. Acad. Sci. U. S. A. 95 (26) (1998) 15671–15676.

[40] Y.R. Lee, S.H. Kweon, K.B. Kwon, J.W. Park, T.R. Yoon, B.H. Park, Inhibition of IL-1beta-mediated inflammatory responses by the IkappaB alpha super-repressor in human fibroblast-like synoviocytes, Biochem. Biophys. Res. Commun. 378 (1) (2009) 90–94.

[41] T. Okamoto, NF-kappaB and rheumatic diseases, Endocr Metab Immune Disord Drug Targets 6 (4) (2006) 359–372.

[42] G.E. Martinez-Bonilla, J.F. Munoz-Valle, V. Delgado-Rizo, B.T. Martin-Marquez, S.L. Ruiz-Quezada, C.R. Best-Aguilera, L. Herrera-Zarate, M. Vazquez-Del Mercado, Placental cytokine expression and NF-kappaB activity in women with rheumatic diseases, Scand. J. Rheumatol. 35 (2) (2006) 160–162.

[43] W. Wang, W. Sun, L. Jin, Caffeic acid alleviates inflammatory response in rheumatoid arthritis fibroblast-like synoviocytes by inhibiting phosphorylation of IkappaB kinase alpha/beta and IkappaBalpha, Int. Immunopharmacol. 48 (2017) 61–66.

[44] I.A. Schepetkin, et al., Anti-Inflammatory Effects and Joint Protection in Collagen-Induced Arthritis after Treatment with IQ-1S, a Selective c-Jun N-Terminal Kinase Inhibitor, J. Pharmacol. Exp. Ther. 353 (3) (2015) 505–516, https://doi.org/10.1124/jpet.114.220251.

[45] N. Haleagrahara, K. Hodgson, S. Miranda-Hernandez, S. Hughes, A.B. Kulur, N. Ketheesan, Flavonoid quercetin-methotrexate combination inhibits inflammatory mediators and matrix metalloproteinase expression, providing protection to joints in collagen-induced arthritis, Inflammopharmacology 26 (5) (2018) 1219–1232, https://doi.org/10.1007/s10787-018-0464-2.

[46] S. Chirumbolo, G. Bjorklund, Quercetin in collagen-induced arthritis. Some comments, Int. Immunopharmacol. 62 (2018) 335–336.

[47] T. Fan, F. Zhong, R. Liu, Y.H. Chen, T. Wang, Q. Ruan, siRNA-mediated c-Rel knockdown ameliorates collagen-induced arthritis in mice, Int. Immunopharmacol. 56 (2018) 9–17.

[48] A. Gul, B. Kunwar, M. Mazhar, S. Faizi, D. Ahmed, M.R. Shah, S.U. Simjee, Rutin and rutin-conjugated gold nanoparticles ameliorate collagen-induced arthritis in rats through inhibition of NF-kappaB and iNOS activation, Int. Immunopharmacol. 59 (2018) 310–317.